Nano Energy 47 (2018) 43–50

Contents lists available at ScienceDirect

Nano Energy

journal homepage: www.elsevier.com/locate/nanoen

Full paper

Suppressing self-discharge of supercapacitors *via* electrorheological effect of liquid crystals

Mengyang Xia[a,b], Jinhui Nie[a,b], Zailei Zhang[a,b], Xianmao Lu[a,b,c,*], Zhong Lin Wang[a,b,c,d,*]

[a] Beijing Institute of Nanoenergy and Nanosystems, Chinese Academy of Sciences, Beijing 100083, PR China
[b] College of Nanoscience and Technology, University of Chinese Academy of Sciences, Beijing 100049, PR China
[c] CAS Center for Excellence in Nanoscience, National Center for Nanoscience and Technology (NCNST), Beijing 100190, PR China
[d] School of Materials Science and Engineering, Georgia Institute of Technology, Atlanta, GA 30332-0245, USA

ARTICLE INFO

Keywords:
Supercapacitors
Self-discharge
Electrorheological effect
Liquid crystals

ABSTRACT

For electric double layer capacitors (EDLCs, or supercapacitors), self-discharge has been an inevitable issue that causes decay of cell voltage and loss of stored energy, but this problem has long been ignored in the studying of supercapacitors. Due to self-discharge, applications of supercapacitors for long-term energy storage or collecting environmental energy harvested by small power devices have been severely limited. There are three main self-discharge processes for EDLCs, including i) charge diffusion and redistribution, ii) faradaic reactions, and iii) ohmic leakage. In this work, we introduced a nematic liquid crystal 4-n-pentyl-4′-cyanobiphenyl (5CB) as an additive to the electrolyte to suppress the self-discharge of EDLCs. When the EDLCs are charged, the electric field in the double layers near the electrode surface induces alignment of 5CB molecules, causing much enhanced fluid viscosity via the so-called electrorheological (ER) effect. As a result, the diffusion of ions and redox species in the electrolyte can be impeded and the self-discharge rate can be reduced. Here, we have demonstrated that by adding 2% of 5CB in $TEMABF_4$/acetonitrile electrolyte, the decay rate of open circuit potential and leakage current can be reduced by more than 80%. Simulation results confirmed the reduced contribution of both diffusion of ions and faradaic reactions to the overall self-discharge. Furthermore, when 5CB EDLCs were employed for storing energy harvested by a triboelectric nanogenerator (TENG) that has a characteristic of pulsed output current, much enhanced charging efficiency was attained compared to EDLCs without 5CB. Our study pointing to a feasible way for truly pushing supercapacitor for practical applications.

1. Introduction

Supercapacitors as an important class of electric energy storage devices exhibit distinct advantages of long cycling lifetime, high charging and discharging rates, as well as superior safety [1–5]. However, applications of supercapacitors are mainly limited to short-term energy storage due to the self-discharge processes that cause substantial voltage decay, leakage current, and loss of stored energy [2,6,7]. Particularly, when supercapacitors are employed to store environmental energy harvested *via* small power devices such as piezoelectric or triboelectric nanogenerators, the relatively large leakage current of supercapacitors compared to that delivered by nanogenerators may result in low charging efficiency and prolonged charging time to reach full capacity [8–16].

Charged supercapacitors are in their high energy state, and Gibbs free energy is the thermodynamic driving force for self-discharge [17]. For supercapacitors based on electric double layer mechanism (or electric double layer capacitors, EDLCs), there are three main self-discharge processes: charge redistribution [17–28], faradaic reactions [17,18,22,27,29–31], and ohmic leakage [17,18,22,27]. Charge redistribution is caused by the movement or loss of charged ions adsorbed on the electrode due to concentration gradient [21,26,28]. Faradaic reaction process describes the oxidation or reduction of redox species on the electrode surface caused by overcharging or presence of impurities [17,18,22,30,31]. Ohmic leakage occurs due to the internal ohmic leakage pathways between the positive and negative electrodes [17,18,22]. All these self-discharge processes will lead to reduced open circuit potential (OCP) and loss of stored energy of charged EDLCs.

To date, various approaches have been adopted to alleviate the self-discharge of supercapacitors by modifying the electrode, separator, or electrolyte. For instance, Tevi et al. developed a method to form an insulating layer on the EDLC electrode by depositing an ultra-thin poly (p-phenylene oxide) to reduce the leakage current [32]. They found that after 1 h of self-discharge, the OCP of the EDLC dropped from 2.0 V

* Corresponding author at:.
E-mail addresses: luxianmao@binn.cas.cn (X. Lu), zlwang@gatech.edu (Z.L. Wang).

https://doi.org/10.1016/j.nanoen.2018.02.022
Received 9 November 2017; Received in revised form 31 January 2018; Accepted 12 February 2018
Available online 21 February 2018
2211-2855/

to 1.44 V. Chen and coworkers employed ion-exchange membranes as the separator to suppress the self-discharge caused by redox active species [33]. Their result showed that the OCP dropped from 0.8 V to 0.3 V in 1.3 h, while the supercapacitors with typical cellulose acetate separator dropped to 0.3 V after 0.4 h. Fic et al. added surfactants into the electrolyte to reduce the self-discharge rate. They propose that because of the long alkyl chain, surfactants adsorbed on the electrode surface should serve as a micro-insulator and hinder the flow of discharge current [34]. Based on this method, they showed that after 20 h the OCP of the supercapacitors dropped from 0.8 V to 0.5 V, while the OCP of the blank samples without surfactants dropped to 0.176 V.

Despite the current progress in reducing self-discharge of supercapacitors, it is still imperative to develop simple and effective strategies to further reduce the self-discharge and improve their applications for environmental energy harvesting and storage. In this work, we report a new approach to reduce self-discharge of supercapacitor based on electrorheological (ER) effect. We have found that the self-discharge of EDLCs can be effectively suppressed by introducing ER molecules such as 4-n-pentyl-4′-cyanobiphenyl (5CB) into the electrolyte. 5CB is a nematic liquid crystal which shows high dielectric anisotropy and chemical stability. When an electric field is applied, 5CB molecules undergo directional alignment with their long axes roughly parallel to each other. The change in molecular order can cause drastically enhanced fluid viscosity that is tunable via the external electric field. This phenomenon is called electrorheological effect [35,36]. When an EDLC is charged, electric double layers (EDLs) form at its electrode-electrolyte interfaces [18,37]. The field strength within the double layer should be strong enough to induce ER effect if liquid crystal modules exist within the double layer. Indeed, Abbott and coworkers have demonstrated such alignment of 5CB molecules within an EDL [38,39]. Sato et al. also reported tunable ionic conductivity of liquid crystal electrolytes by controlling the formation of an EDL [40]. Therefore, we expect that by introducing 5CB in the EDLC electrolyte, the fluid viscosity in the EDL should increase when the capacitor is charged, resulting in much slower diffusion. Due to the reduced diffusivity of ions, charge re-distribution on the electrode surface and diffusion of ions away from the EDL will be hindered, leading to reduced leakage current and suppressed self-discharge (Fig. 1). Electrochemical tests indicate that with 5CB in the electrolyte, the EDLC showed a much smaller leakage current of 2.2 μA compared to the EDLC without 5CB (12 μA). The decay of open circuit potential of the 5CB EDLC was also significantly reduced – it took 16.5 h for the 5CB EDLC to drop from 2 V to 1.5 V; while for the EDLC without 5CB, the OCP dropped to 1.5 V within only 2.2 h. Moreover, we employed a triboelectric nanonenergator (TENG) to charge the 5CB EDLC and demonstrated much improved charging efficiency due to its small leakage current. The results obtained in the work indicate that the self-discharge of EDLCs may be substantially suppressed by introducing additives that exhibit ER effect in the electrolyte; and improved charging efficiency using small-power energy harvesting devices can be attained. This study points a new approach for largely reduce the self-discharging of supercapacitors.

2. Experimental section

EDLCs were fabricated using 2032 coin cells. A uniform slurry containing activated carbon (Kuraray YP-50F), acetylene black and carboxymethyl cellulose (CMC) at a weight ratio of 70:20:10 was bladed on Al and Cu foils as positive and negative electrodes, respectively. The foils were then heated at 120 °C for 12 h under vacuum to dehydrate thoroughly. The electrolyte was 1 M triethylmethylammonium tetrafluoroborate ($TEMABF_4$) in acetonitrile (Capchem Co., Ltd.). Liquid crystal 4-n-pentyl-4′-cyanobiphenyl (5CB, Aladdin) was added to the electrolyte at a volume ratio of 1:49 (2 vol%). Cellulose paper (NKK TF4840) was used as the separator. All coin cells were assembled in an argon-filled glovebox with oxygen below 0.5 ppm and water below 0.1 ppm. EDLCs without 5CB in the electrolyte were also fabricated as the same process. The areal loadings of activated carbon were 1.4 and 1.2 mg/cm^2 for 5CB and blank EDLCs, respectively. The volume of the electrolyte was 80 μL.

Cyclic voltammograms (CV) and galvanostatic charge-discharge (GCD) curves were obtained on a potentiostat (CHI660E). Self-discharge and cycling stability tests were carried out on a LAND CT2001A battery test system. Electrochemical impedance spectroscopy (EIS) was acquired by a Solartron 1287 A potentiostat in conjunction with a Solartron 1260 A impedance analyzer over a frequency range from 1 MHz to 0.1 Hz at an AC amplitude of 10.0 mV. Raman spectroscopy was performed on a Horiba LabRAM HR Evolution Raman system using an argon ion laser (532 nm) as the excitation source. UV–Vis absorption spectra were obtained on a SHIMADZU UV3600 UV–VIS–NIR Spectrophotometer with a spectral region from 250 nm to 700 nm.

3. Results and discussion

The supercapacitors tested in this work were prepared using activated carbon as the electrode material. For blank samples, 1 M $TEMABF_4$ in acetonitrile solution was used as the electrolyte, but for 5CB samples, we added 5CB (2 vol%) in the electrolyte. Prior to self-discharge test, cyclic voltammetry (CV) and galvanic charge-discharge (GCD) measurements were performed to ensure the devices have the same capacitance. As shown in Fig. 2a-b, GCD results of the blank and 5CB supercapacitors revealed nearly the same charging and discharging profiles at all currents ranging from 0.5 to 10 mA, indicating similar

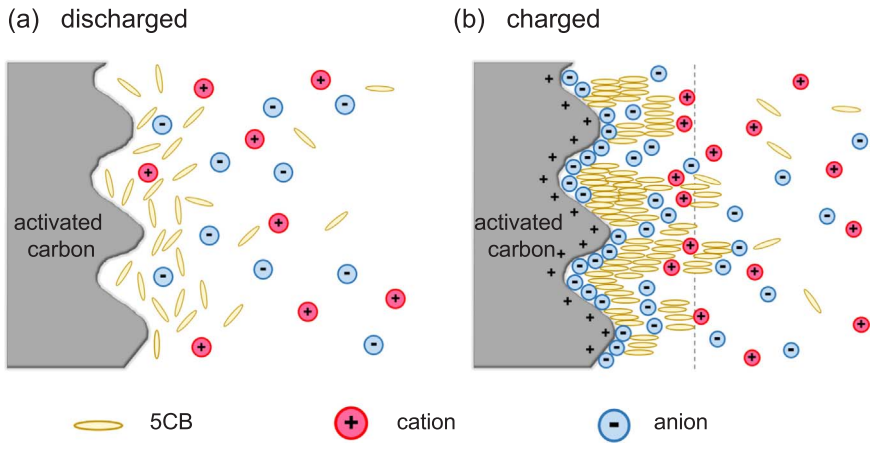

Fig. 1. The electrode-electrolyte interface of an EDLC with 5CB added in the electrolyte. (a) At discharged state, the cations, anions and 5CB molecules in the electrolyte are distributed evenly. (b) When the electrode is charged, the electric field near the electrode surface causes 5CB molecules to align towards the field and enhances flow viscosity.

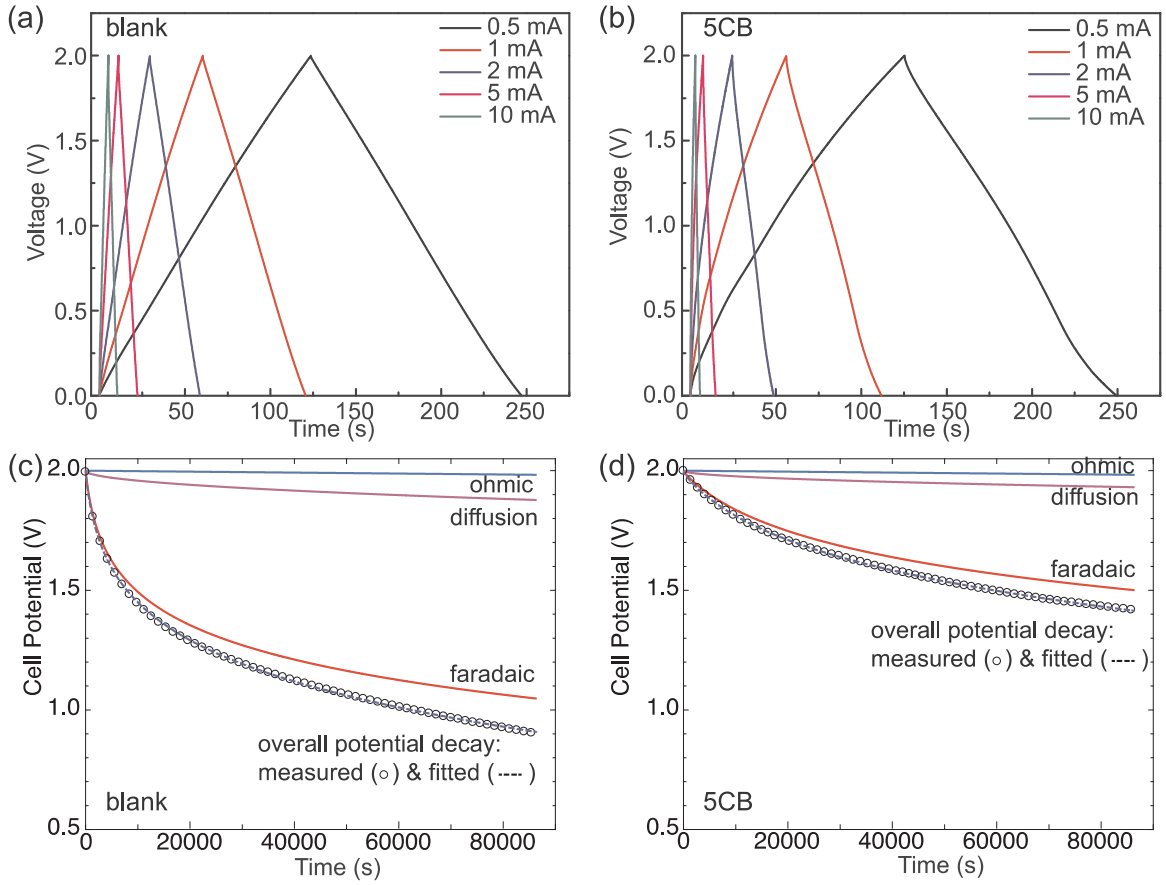

Fig. 2. (a-b) Charge-discharge curves of blank and 5CB EDLCs at different charging currents from 0.5 to 10 mA. (c-d) Decay of open circuit potential for blank and 5CB EDLCs and simulated contributions due to ohmic, diffusion and faradaic leakage.

capacitive behavior of the devices with or without 5CB in the electrolyte. Based on discharging time at 0.5 mA, the capacitances of both blank and 5CB supercapacitors were calculated to be 0.031 F. Their similar capacitive behavior was also confirmed from the CV scans at different scan rates (Fig. S1). Within the voltage range of 0–2 V, the blank sample showed a nearly rectangular CV, typical for an activated carbon-based EDLC with organic electrolyte. For the EDLC with 5CB in the electrolyte, the CV also maintained a pseudo-rectangular shape, although slight deviation from that of the blank EDLC was observed. At the same scan rates, the areas enclosed by the CVs of both samples are nearly the same, indicating the same capacitance for both 5CB and blank EDLCs. In addition, the 5CB EDLC exhibited excellent cycling stability and coulombic efficiency (Fig. S2).

For a charged supercapacitor, the decay of OCP is the most important parameter to characterize its self-discharge process. Fig. 2c-d show the decay of OCP in 24 h for the blank and 5CB EDLCs after the devices were charged to 2 V at a current of 0.2 mA. To ensure the supercapacitors were fully charged, the devices were held at 2 V for 2 h. Although in some reported work much longer holding times such as 24 h have been adopted before self-discharge test [20,21,28], for the interest of practical applications where fast switch between charging and discharging are of immense importance, we chose 2 h of holding time in this work before the applied voltage was removed and the OCPs were monitored. As shown in Fig. 2c, within 2.2 h, the OCP of the blank EDLC dropped to 1.5 V, which is a commonly acceptable voltage for powering electronic devices. While for the 5CB EDLC, it took 16.5 h for its OCP to drop to 1.5 V, six times longer than that of the blank EDLC. The much-prolonged time for the OCP of 5CB EDLC to fall to 1.5 V indicates significantly suppressed self-discharge after adding 5CB in the electrolyte. After 24 h, the OCP of the blank EDLC decreased to 0.90 V. This decrease in OCP corresponds to a significant loss in stored energy of 80%, considering that the energy stored in an EDLC is $E = ½ CV^2$. For the 5CB EDLC, after 24 h the OCP decreased to 1.42 V, which is still considered as a usable voltage for electronic devices. The corresponding loss in stored energy of the 5CB EDLC is ~49.6%, much less than the blank sample. It should be noted that due to the different systems (including electrode materials, electrolytes, separators, and initial cell voltages) employed by researchers for self-discharge tests, it is difficult to benchmark the self-discharge rates of various approaches. However, by examining the OCP decay rates ($\Delta U/\Delta t$) reported in the literature [32–34,41–53], we found that our method of reducing the self-discharge of EDLCs is among the most effective ones (Table S1).

For EDLCs, three self-discharge mechanisms have been proposed: 1) ohmic leakage through a resistance R present in the system in the similar way as a dielectric capacitor; 2) diffusion of adsorbed ions from the surface of the electrode materials leading to charge redistribution or departure of ions from the electric double layer; 3) faradaic process due to overcharge of a supercapacitor or presence of impurities that induce charge transfer reactions at the electrodes.

For ohmic leakage, the voltage change with discharge time t is given as [6,17,27]:

$$U = U_0 \exp\left(-\frac{t}{RC}\right) \quad (1)$$

where U_0 is the initial potential of the charged supercapacitor (2 V in this work), C is the capacitance of the device, and RC corresponds to the time constant of the self-discharge process.

For diffusion-controlled variation of ion concentration, the corresponding voltage drop is proportional to $t^{1/2}$ [17,27,30]:

$$U = U_0 - m\sqrt{t} \quad (2)$$

where m is called diffusion parameter that represents the diffusion rate

of the ions near the electrode surface.

Due to overcharging of a supercapacitor or the presence of impurities such as Fe^{3+}, Cl^-, and free acids in the electrolyte, species that can form redox shuttles diffuse between the two electrodes and can be reduced or oxidized. As a result, the charge transfer reactions of the redox shuttles reduce the voltage of the device. Based on Bultler-Volmer equation, the voltage change due to faradaic reactions can be described as [6,17,27,54]:

$$U = U_0 - \frac{RT}{\alpha F}\ln\frac{\alpha F i_0}{RTC} - \frac{RT}{\alpha F}\ln\left(t + \frac{CK}{i_0}\right) \quad (3)$$

where α is charge transfer coefficient, T is temperature, R is ideal gas constant, F is Faradaic constant, i_0 is exchange current, and K is an integration constant.

Combining the potential decays caused by all three mechanisms, the following general formula can be used to simulate the self-discharge curve $U = f(t)$ [27]:

$$U = U_0\exp\left(-\frac{t}{RC}\right) - m\sqrt{t} - a - b\ln(t + \frac{CK}{i_0}) \quad (4)$$

where a, b are constants related to the faradaic process.

Based on the above equation, the simulated OCP *vs.* t for both blank and 5CB EDLCs were obtained and the results are superimposed on the measured OCP curves as shown in Fig. 2c-d. It is clear that there is a perfect match between the simulated and measured OCP drop over the whole test period. The OCP decay caused by each individual self-discharge mechanism, i.e., the exponential decay due to ohmic leakage, the diffusion decay that is proportional to $\sqrt{t}$, and the faradaic reaction decay that is proportional to $\ln(t)$, was also plotted. Compared to the decay caused by faradaic reaction and diffusion, the ohmic decay is much smaller, primarily due to the large leakage resistance R present in the system. It is evident that the faradaic and diffusion processes led to much larger potential decay of the blank EDLC than that of the 5CB sample, indicating much suppressed self-discharge for the supercapacitor with 5CB in the electrolyte. The diffusion parameters, m, of both EDLCs were estimated based on the simulation results. For the blank EDLC, the diffusion parameter is 4.2×10^{-4} V/sec. $^{1/2}$, close the reported value for EDLCs with activated carbon electrode and organic electrolyte [30]. For 5CB EDLC, the estimated diffusion parameter is 2.3×10^{-4} V/sec. $^{1/2}$, about half that of the blank EDLC. The much smaller diffusion parameter of the 5CB EDLC implies reduced diffusion of ions, thereby causing slower loss of charges from the double layer. In addition to the diffusion process, the potential drop due to the faradaic process was also reduced after adding 5CB in the electrolyte. This is not surprising since when 5CB molecules in the electric double layer induce sluggish ion diffusion, the transfer of redox couples between the electrodes should be hindered as well. As a result, the rate of the electrochemical reaction of impurities at the electrode surface should be reduced. Therefore, it is evident that the use of 5CB in the electrolyte not only led to slower diffusion of ions but also reduced charge transfer reactions of redox shuttles at the electrode surface - both effects are beneficial to the suppression of self-discharge.

Based on the above results, it is clear that by adding a small amount of 5CB (2 vol% or 0.08 M), the self-discharge process of the EDLC can be dramatically suppressed. 5CB as a type of liquid crystal possess anisotropic dielectric properties. the orientation of 5CB molecules can be controlled by electric field, leading to the so-called electrorheological effect that causes considerately increased fluid viscosity. The change in fluid viscosity and the alignment of molecules within the electric field will impede the diffusion of dissolved ions. For a charged supercapacitor, the electric field within the double layers can be as high as

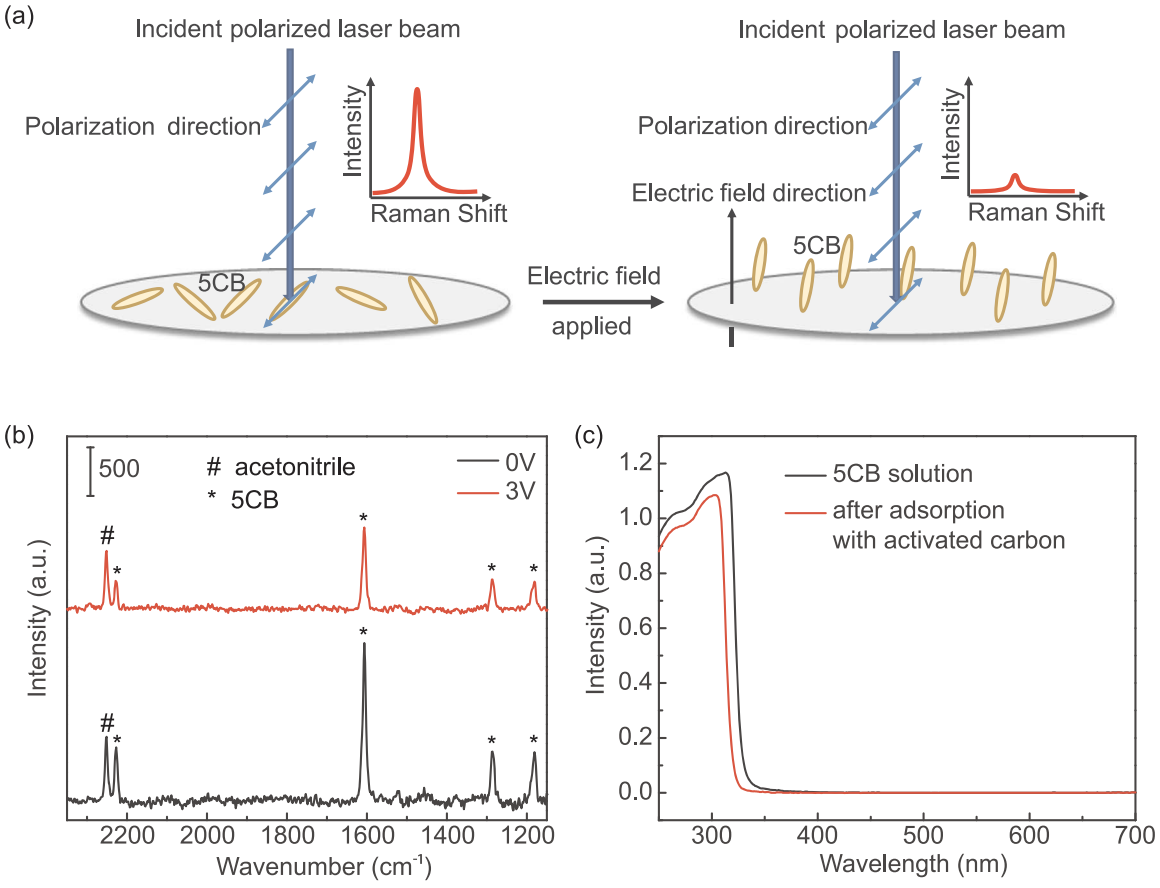

Fig. 3. (a) Schematic illustration of the change in Raman intensity for 5CB molecules at different orientations. (b) Raman spectra of 5CB dissolved in acetonitrile with and without applied electric field. (c) UV–Vis absorption spectra of 5CB in acetonitrile solution before and after treated by activated carbon.

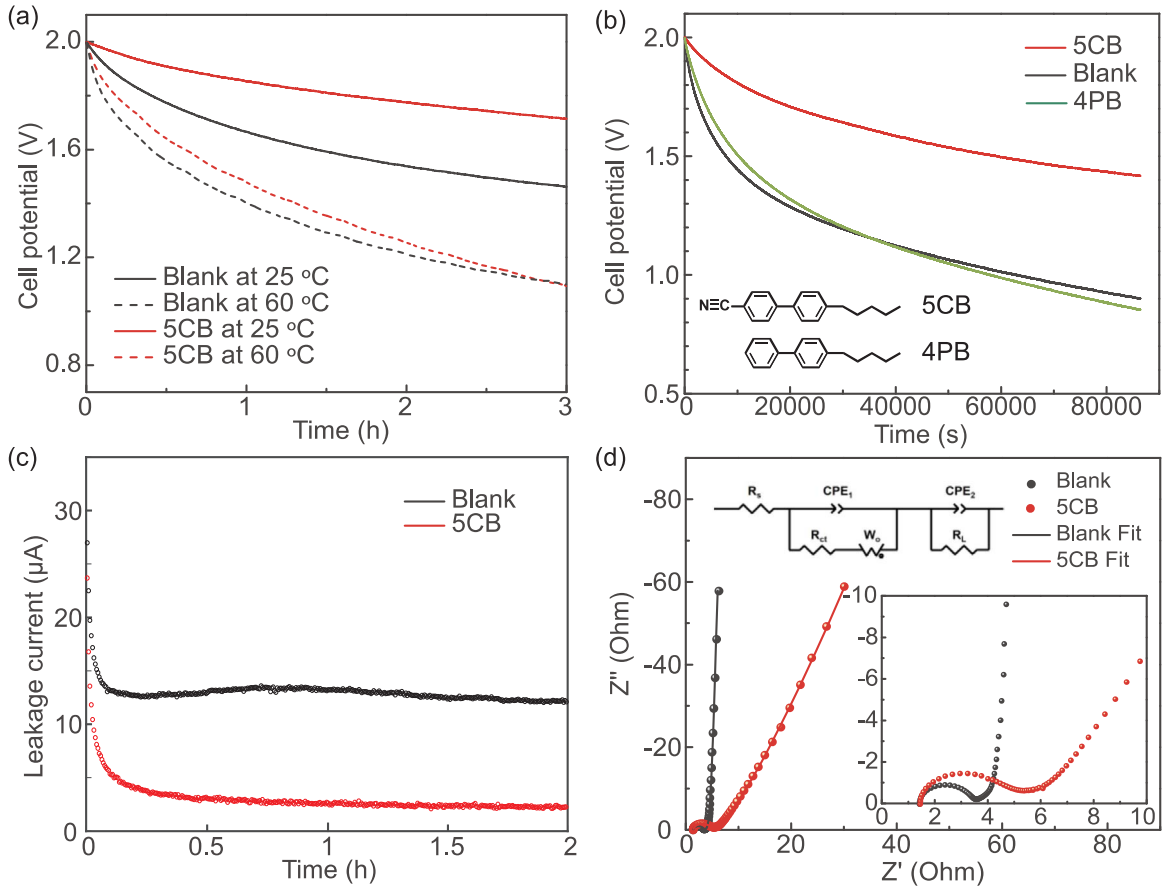

Fig. 4. (a) Decay of OCP for blank and 5CB EDLCs at room temperature and 60 °C. (b) Comparison of OCP decay for 5CB, 4PB, and blank EDLCs. (c) Leakage currents of blank and 5CB EDLCs at 2 V. (d) EIS of blank and 5CB EDLCs.

10^9 V/m, much larger than the required electric field to induce directional alignment of liquid crystal molecules. In fact, both theoretical and experimental studies have proved that liquid crystal molecules such as 5CB can change orientations within an electric double layer. For example, 5CB molecules can be oriented either parallel or vertical to the surface of an electrode by tuning the electric field within a double layer that is formed by chemisorbed HS-$(CH_2)_{10}$COONa on electrode through pH tunning [39]. When 5CB molecules are vertically aligned with respect to the electrode surface, the fluid rheological properties would change and reduce the diffusion of ions and redox species within the double layer. Consequently, slower charge redistribution and charge transfer reactions at the electrodes are expected. Therefore, the self-discharge rate can be much reduced. When the EDLC is discharged and the electric field is removed, the driving force for the vertical alignment of 5CB molecules disappears and the diffusion of ions and redox species in the electrolyte will be restored.

In order to demonstrate the alignment of 5CB molecules under electric field, we carried out confocal Raman spectroscopy measurements. Raman spectroscopy is a characterization technique that detects vibrational modes of specific chemical groups [55]. The spectral intensities can reveal the spatial organization and local environment of the molecules [56]. It has been reported that different orientations of 5CB molecules near an electrode surface can be detected by polarized confocal Raman spectroscopy [39,55]. Because Raman signals cannot pass activated carbon electrodes, we used a transparent cell fabricated with two pieces of FTO glass for the Raman measurements. The cell was filled with 5CB dissolved in 1 M $TEMABF_4$ in acetonitrile solution. The distance between the two pieces of FTO was about 50 μm, so that a strong electric field could be created when a relative low direct current (DC) voltage of 3 V was applied between the two pieces of FTO. The wavelength of the incident laser was 532 nm and the Raman spectra were collected between 2350 and 1150 cm^{-1}. Higher Raman intensity is expected when the incident plane polarized light vector is along the axes of 5CB molecules, while a lower intensity should be obtained when the polarized light vector is perpendicular to the axes of 5CB molecules (Fig. 3a) [55,57]. Fig. 3b shows the Raman spectra of the FTO cell at two applied voltages, 0 V and 3 V, respectively. There are five peaks in each spectrum. The solvent, acetonitrile, showed one peak at 2251 cm^{-1} corresponding to the C≡N stretch. The other four peaks at 2228, 1606, 1286, and 1180 cm^{-1} can be attributed to 5CB molecules corresponding to C≡N stretch, C-C stretch of aromatic ring, C-C stretch of biphenyl link, and C-H in-plane deformation, respectively. For the spectra obtained at 0 and 3 V, the intensity of the acetonitrile peak at 2251 cm^{-1} remained almost the same. This is expected since with or without applied voltages, the spatial arrangement and local chemical environment of the solvent molecules should remain largely unchanged. However, the intensities all 5CB characteristic peaks decreased when a voltage of 3 V was applied, indicating that the orientation of 5CB molecules changed under electric field. At 0 V, 5CB molecules should lay flat on the electrode surface, with an orientation that is parallel to the polarized direction of the incident laser to give high Raman peak intensity. According to the decrease of Raman intensity, the orientation of 5CB changed from parallel to vertical to the electrode surface when a voltage was applied. From this point of view, 5CB molecules can align vertically to the electrode surface and restrain the movement of charged ions through increased fluid viscosity, thus slowing down the self-discharge of EDLCs.

It should be noted that the concentration of 5CB for the Raman measurement was 50 vol%, much higher than 2% used in the electrolyte of the EDLCs. In a diluted solution, the alignment of 5CB under

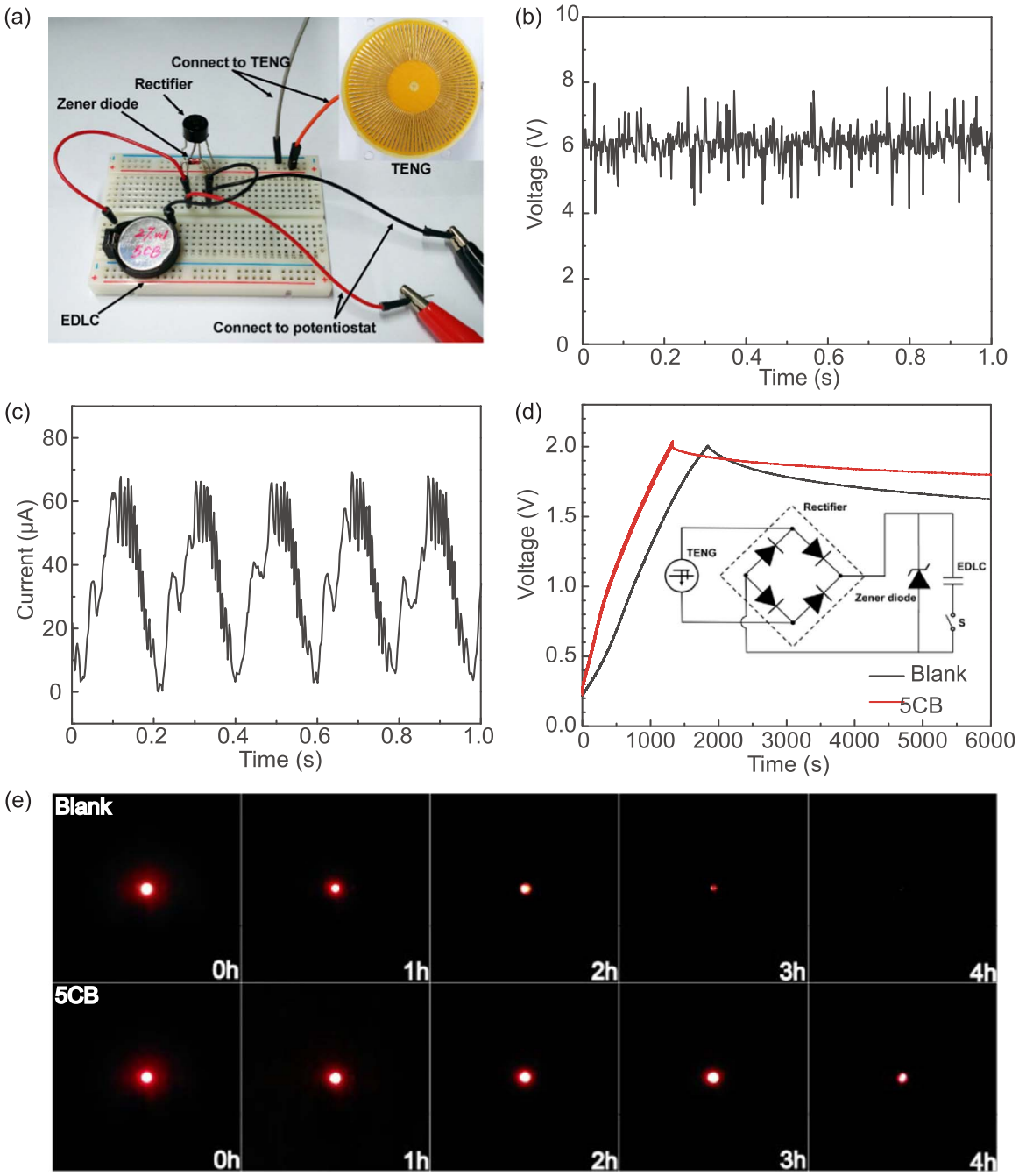

Fig. 5. (a) Circuit used to charge Blank and 5CB EDLCs with a TENG. (b-c) Open circuit voltage and short circuit current provided by the TENG after a bridge rectifier and a Zener diode. (d) Charge/self-discharge curves of the EDLCs. Inset shows the circuit diagram of the power system. (e) LED lights powered by blank and 5CB EDLCs, before lighting the LEDs, the EDLCs were charged to 2 V and subjected to self-discharge of 0, 1, 2, 3 and 4 h.

electric field may not be observed due to the much-reduced intermolecular interaction. Although the electrolyte of the supercapacitors in our discharge test contains diluted 5CB, due to surface adsorption, 5CB should be concentrated near activated carbon surface and may reach the concentration that exhibits electrorheological effect in the EDLC. To confirm the enrichment effect of 5CB on the electrode, we conducted UV–Vis absorbance measurements to examine the change in concentration of 5CB in the electrolyte after surface adsorption with activated carbon. As shown in Fig. 3c, it is clear that the UV–vis absorption peak intensity of 0.2% 5CB solution was reduced after being treated with activated carbon, indicating an appreciable amount of 5CB molecules were adsorbed by activated carbon. Therefore, in 5CB EDLC, the concentration of 5CB should be much higher near the activated carbon electrode than the bulk solution. Therefore, the alignment of 5CB molecules near the electrode surface can still be afforded under electric field.

The alignment of nematic LC molecules only occurs within a certain temperature range. For 5CB, its nematic phase exists between 23 °C and 35 °C, above which 5CB transforms into isotropic phase and the molecular orientation will not be controlled by electric field [36]. Therefore, we expect that at elevated temperatures the effect of self-discharge suppression caused by 5CB should disappear. To confirm that, we carried out self-discharge test at 60 °C, a temperature beyond the isotropic phase transformation of 5CB. As shown in Fig. 4a, much faster self-discharge rates were observed at 60 °C for both blank and 5CB EDLCs. This is expected since at higher temperatures, both ion diffusion and

charge transfer reactions will be accelerated [21,58,59]. More interestingly, the self-discharge rates of EDLCs with and without 5CB became almost equal at 60 °C. The OCPs of both devices dropped from 2 V to 1.1 V after around 3 h, indicating that adding 5CB to the electrolyte cannot reduce the self-discharge at temperatures higher than the isotropic transformation point. This result confirms that the slower self-discharge of 5CB EDLC should be attributed to the directional alignment of 5CB under the electric field of the double layer.

To further confirm our hypothesis, we performed a control experiment by replacing 5CB with another molecule, 4-n-pentylbiphenyl (4PB), as an additive to the electrolyte. The molecular structures of 4PB and 5CB are similar (Fig. 4b), except that 4PB does not show electrorheological effect due to the absence of cyano group. The OCP decay of 4PB EDLC was presented in Fig. 4b. By adding 4PB in the electrolyte, the EDLC exhibited similar self-discharge rate compared to that of the blank EDLC, indicating that adding molecules without electrorheological effect in the electrolyte did not suppress the self-charge of EDLCs.

In addition to potential decay, leakage current is another important self-discharge parameter of EDLCs. After the EDLCs were charged, the leakage currents, corresponding to the applied currents to maintain the charged potential, were recorded by holding the devices at 2 V (Fig. 4c). For both blank and 5CB EDLCs, the initial leakage currents were high due to the fast discharge process at the beginning. After 1.5 h, the leakage current of the blank EDLC stabilized at 12 μA. For 5CB EDLC, the leakage current after 1.5 h was 2.2 μA, which was significantly reduced (by 82%) relative to the blank EDLC.

The electrochemical impedance spectra (EIS) of the EDLCs with and without 5CB are shown in the Fig. 4d. All of the curves display two parts: a compressed semicircle at the high frequencies shows the charge transfer resistance and constant phase element of the electrodes, and a sloping line following the semicircle at the low frequencies reflects the diffusion of ions in the porous electrode. The inset in Fig. 4d exhibits the equivalent circuit, where R_s, R_{ct}, R_L, *CPE*, W_o represent the resistance of the electrolyte, charge transfer resistance, leakage resistance, double layer capacitance, Warburg impedance, respectively. The simulated R_L values of both blank and 5CB samples are very high, consistent with the low ohmic leakage based on self-discharge test.

Suppressing the self-discharge of supercapacitors is of particular importance for harvesting and storing ambient energy provided by the environment. This is because environmental energy harvesting devices based on piezoelectric, thermal, vibrational, or triboelectric mechanism can only deliver small power at mW or μW scale. Therefore, their connected energy storage devices would be charged at electric currents of μA level. Any reduction of the leakage current at μA should considerably enhance the energy storage efficiency and reduce charging time. To demonstrate the difference in harvesting and storing ambient energy between the blank and 5CB EDLCs, we employed a triboelectric nanogenerator (TENG) to charge the supercapacitors. The TENG we used is a radial arrayed triboelectric generator, as is shown in the inset of Fig. 5a. The TENG consists of a stator and a rotator which was driven by a rotary motor. The measured open circuit voltage and peak short circuit current after a bridge rectifier and Zener diode were about 6 V and 60 μA, respectively (Fig. 5b-c). Fig. 5d shows the charging process powered by the TENG and the decay of OCPs after the EDLCs were charged. For blank EDLC, it took ~30 min to charge to 2.0 V, while for 5CB EDLC, it took ~20 min. Once the EDLCs were charged to 2.0 V, the TENG was disconnected from the circuit and the EDLCs were kept in an open circuit condition to measure the self-discharge rates. Obviously, the self-discharge of 5CB EDLC is much lower than the blank EDLC. The faster and more efficient charging process of 5CB EDLC benefits considerably from its smaller leakage current.

Similar to the charging process, when supercapacitors are employed to drive small-power devices, the period of continuous power supply can be extended for supercapacitors with low self-discharge rate. As shown in the video (Supporting Information), when blank and 5CB EDLCs charged at 2 V were used to drive LCD timers, the 5CB EDLC continuously powered the timer for 1 h and 40 min before its LCD faded out. But for the blank EDLC, the timer only lasted for ~1 h. LED lights were also employed to show the prolonged energy storage from the 5CB EDLC with suppressed self-discharge. As shown in Fig. 5e, after 4 h of self-discharge, the 5CB EDLC still lit the LED brightly, but the blank EDLC failed to light the LED after 3 h.

Supplementary material related to this article can be found online at http://dx.doi.org/10.1016/j.nanoen.2018.02.022.

4. Conclusions

In this work, we have demonstrated that self-discharge of EDLCs can be effectively suppressed by introducing ER liquid crystal molecules in the electrolyte. The enhanced fluid viscosity governed by the ER effect causes slow diffusion of ions in a charged EDLC. Therefore, two main pathways for self-discharge, charge redistribution and faradaic reactions, can be much reduced. With 5CB liquid crystal as an example, we showed that after adding small amount of 5CB in $TEMABF_4$/acetonitrile electrolyte of an EDLC, the decay rate of OCP and leakage current can be drastically reduced by more than 80%. The suppressed self-discharge of 5CB EDLCs not only improved the charging efficiency from environmental energy harvesting devices such as TENGs, but also facilitated prolonged power supply for driving small power devices.

Acknowledgment

The authors thank the National Key R & D Project from Ministry of Science and Technology, China (Grant No. 2016YFA0202701) and “Thousands Talents” Program (China) for the pioneer researcher (Z.L.W.) and his innovation team and the for support.

Appendix A. Supplementary material

Supplementary data associated with this article can be found in the online version at http://dx.doi.org/10.1016/j.nanoen.2018.02.022.

References

[1] G. Wang, L. Zhang, J. Zhang, Chem. Soc. Rev. 41 (2012) 797–828.
[2] C. Zhong, Y. Deng, W. Hu, J. Qiao, L. Zhang, J. Zhang, Chem. Soc. Rev. 44 (2015) 7484–7539.
[3] P. Simon, Y. Gogotsi, Nat. Mater. 7 (2008) 845–854.
[4] P. Simon, Y. Gogotsi, B. Dunn, Science 343 (2014) 1210–1211.
[5] J.R. Miller, P. Simon, Science 321 (2008) 651–652.
[6] I.S. Ike, I. Sigalas, S. Iyuke, Phys. Chem. Chem. Phys. 18 (2016) 661–680.
[7] G. Xiong, C. Meng, R.G. Reifenberger, P.P. Irazoqui, T.S. Fisher, Electroanalysis 26 (2014) 30–51.
[8] Z.L. Wang, J. Song, Science 312 (2006) 242–246.
[9] X. Wang, J. Song, J. Liu, Z.L. Wang, Science 316 (2007) 102–105.
[10] Y. Qin, X. Wang, Z.L. Wang, Nature 451 (2008) 809–813.
[11] Z.L. Wang, ACS Nano 7 (2013) 9533–9557.
[12] S. Wang, L. Lin, Z.L. Wang, Nano Energy 11 (2015) 436–462.
[13] S.H. Wang, Z.H. Lin, S.M. Niu, L. Lin, Y.N. Xie, K.C. Pradel, Z.L. Wang, ACS Nano 7 (2013) 11263–11271.
[14] J. Wang, X. Li, Y. Zi, S. Wang, Z. Li, L. Zheng, F. Yi, S. Li, Z.L. Wang, Adv. Mater. 27 (2015) 4830–4836.
[15] J. Wang, Z. Wen, Y. Zi, P. Zhou, J. Lin, H. Guo, Y. Xu, Z.L. Wang, Adv. Funct. Mater. 26 (2016) 1070–1076.
[16] Z.L. Wang, J. Chen, L. Lin, Energy Environ. Sci. 8 (2015) 2250–2282.
[17] B.E. Conway, W.G. Pell, T.C. Liu, J. Power Sources 65 (1997) 53–59.
[18] B.E. Conway, Electrochemical Supercapacitors: Scientific Fundamentals and Technological Applications, Kluwer Academic / Plenum Publishers, New York, 1999.
[19] W.G. Pell, B.E. Conway, W.A. Adams, J. de Oliveira, J. Power Sources 80 (1999) 134–141.
[20] J. Black, H.A. Andreas, Electrochim. Acta 54 (2009) 3568–3574.
[21] M. Kaus, J. Kowal, D.U. Sauer, Electrochim. Acta 55 (2010) 7516–7523.
[22] H.A. Andreas, J. Electrochem. Soc. 162 (2015) A5047–A5053.
[23] J. Black, H.A. Andreas, J. Power Sources 195 (2010) 929–935.
[24] Y. Zhang, H. Yang, J. Power Sources 196 (2011) 4128–4135.
[25] H.Z. Yang, Y. Zhang, J. Power Sources 196 (2011) 8866–8873.
[26] C.L. Hao, X.F. Wang, Y.J. Yin, Z. You, J. Electron. Mater. 45 (2016) 2160–2171.
[27] A. Lewandowski, P. Jakobczyk, M. Galinski, M. Biegun, Phys. Chem. Chem. Phys.

15 (2013) 8692–8699.
[28] J. Kowal, E. Avaroglu, F. Chamekh, A. S'Enfelds, T. Thien, D. Wijaya, D.U. Sauer, J. Power Sources 196 (2011) 573–579.
[29] J.J. Niu, W.G. Pell, B.E. Conway, J. Power Sources 156 (2006) 725–740.
[30] B.W. Ricketts, C. Ton-That, J. Power Sources 89 (2000) 64–69.
[31] B. Pillay, J. Electrochem. Soc. 143 (1996) 1806.
[32] T. Tevi, H. Yaghoubi, J. Wang, A. Takshi, J. Power Sources 241 (2013) 589–596.
[33] L.B. Chen, H. Bai, Z.F. Huang, L. Li, Energy Environ. Sci. 7 (2014) 1750–1759.
[34] K. Fic, G. Lota, E. Frackowiak, Electrochim. Acta 55 (2010) 7484–7488.
[35] T. Hao, Adv. Mater. 13 (2001) 1847–1857.
[36] K. Negita, J. Chem. Phys. 105 (1996) 7837–7841.
[37] L. Wei, G. Yushin, Nano Energy 1 (2012) 552–565.
[38] Y.Y. Luk, N.L. Abbott, Science 301 (2003) 623–626.
[39] R.R. Shah, N.L. Abbott, J. Phys. Chem. B 105 (2001) 4936–4950.
[40] K. Sato, T. Yamasaki, T. Mizuma, K. Oyaizu, H. Nishide, J. Mater. Chem. A 4 (2016) 3249–3252.
[41] S. Nohara, H. Wada, N. Furukawa, H. Inoue, C. Iwakura, Res. Chem. Intermed. 32 (2006) 491–496.
[42] K. Fic, G. Lota, E. Frackowiak, Electrochim. Acta 60 (2012) 206–212.
[43] F. Soavi, C. Arbizzani, M. Mastragostino, J. Appl. Electrochem. 44 (2014) 491–496.
[44] Q. Zhang, C. Cai, J.W. Qin, B.Q. Wei, Nano Energy 4 (2014) 14–22.
[45] B. Wang, J.A. Macia-Agullo, D.G. Prendiville, X. Zheng, D. Liu, Y. Zhang, S.W. Boettcher, X. Ji, G.D. Stucky, J. Electrochem. Soc. 161 (2014) A1090–A1093.
[46] S.E. Chun, B. Evanko, X.F. Wang, D. Vonlanthen, X.L. Ji, G.D. Stucky, S.W. Boettcher, Nat. Commun. 6 (2015) 10.
[47] T. Sato, S. Marukane, T. Morinaga, T. Kamijo, H. Arafune, Y. Tsujii, J. Power Sources 295 (2015) 108–116.
[48] J. Wang, B. Ding, X. Hao, Y. Xu, Y. Wang, L. Shen, H. Dou, X. Zhang, Carbon 102 (2016) 255–261.
[49] E. Mourad, L. Coustan, P. Lannelongue, D. Zigah, A. Mehdi, A. Vioux, S.A. Freunberger, F. Favier, O. Fontaine, Nat. Mater. 16 (2017) 446–453.
[50] J. Lee, S. Choudhury, D. Weingarth, D. Kim, V. Presser, ACS Appl. Mater. Interfaces 8 (2016) 23676–23687.
[51] J. Lee, B. Krüner, A. Tolosa, S. Sathyamoorthi, D. Kim, S. Choudhury, K.-H. Seo, V. Presser, Energy Environ. Sci. 9 (2016) 3392–3398.
[52] S.J. Yoo, B. Evanko, X. Wang, M. Romelczyk, A. Taylor, X. Ji, S.W. Boettcher, G.D. Stucky, J. Am. Chem. Soc. 139 (2017) 9985–9993.
[53] J. Lee, A. Tolosa, B. Krüner, N. Jäckel, S. Fleischmann, M. Zeiger, D. Kim, V. Presser, Sustain. Energy Fuels 1 (2017) 299–307.
[54] J.J. Niu, B.E. Conway, W.G. Pell, J. Power Sources 135 (2004) 332–343.
[55] E.A. Buyuktanir, K. Zhang, A. Gericke, J.L. West, Mol. Cryst. Liq. Cryst. 487 (2008) 39–51.
[56] M. Pastorczak, M. Wiatrowski, M. Kozanecki, M. Lodzinski, J. Ulanski, J. Mol. Struct. 744–747 (2005) 997–1003.
[57] W. Jeremy Jones, D.K. Thomas, D.W. Thomas, G. Williams, J. Mol. Struct. 708 (2004) 145–163.
[58] Q. Zhang, J.P. Rong, B.Q. Wei, RSC Adv. 1 (2011) 989–994.
[59] Q. Zhang, J.P. Rong, D.S. Ma, B.Q. Wei, Energy Environ. Sci. 4 (2011) 2152–2159.